

# **MIMO Radar with OTFS Modulation**

*A Project Report*

*Submitted by*

**RAMKUMAR A**

*In partial fulfilment of the requirements  
for the award of the degree of*

**MASTER OF TECHNOLOGY**



**DEPARTMENT OF ELECTRICAL ENGINEERING  
INDIAN INSTITUTE OF TECHNOLOGY MADRAS.**

**JUNE 2021**

## THESIS CERTIFICATE

This is to certify that the thesis titled “**MIMO Radar with OTFS Modulation**”, submitted by **RAMKUMAR A**, to the Indian Institute of Technology, Madras, for the award of the degree of Master of Technology, is a bona fide record of the research work done by him under our supervision. The contents of this thesis, in full or in parts, have not been submitted to any other Institute or University for the award of any degree or diploma.

Prof. Srikrishna Bhashyam  
Project Guide  
Professor  
Dept. of Electrical Engineering  
IIT-Madras, 600 036

Place: Chennai

Date: June 2021

## **ACKNOWLEDGEMENTS**

I am ever thankful to Prof. Srikrishna Bhashyam for his continual support and invaluable advice throughout the duration of my project. I feel honored and encouraged to have worked under his guidance.

I also thank Dr Avhishek chatterjee for his valuable support as a faculty advisor during my entire tenure as a student.

I would like to thank the Department of Electrical Engineering and Indian Institute of Technology Madras for providing an excellent and ideal environment for learning.

Finally, I would like to thank my family and parents for their love, patience and continuous encouragement.

## ABSTRACT

A new 2D modulation scheme referred to as OTFS (Orthogonal Time Frequency & Space) that multiplexes information QAM symbols over new class of carrier waveforms that correspond to localized pulses in delay-Doppler representation can be used simultaneously in radar and communication [1]. In this project, I propose to implement radar moving target detection and parameter estimation problems where the transmitter, equipped with a mono-static MIMO radar, using orthogonal time frequency space (OTFS) modulation based on paper “Hybrid Digital-Analog Beam forming and MIMO Radar with OTFS Modulation [2]. Assuming that the number of radio frequency chains is smaller than the number of antennas over the mm Wave frequency band [2]. The scenario considers a wide angular beam in order to perform the single and multiple moving target detection and parameter estimation. Under this setup, I will develop MATLAB based module like generation of target, OTFS modulation and demodulation, Matched filter (pulse compression) technique combined with hybrid beam forming with different varying phases [2], to jointly perform target detection and radar parameter estimation. Numerical results will demonstrate that the detection of single and multiple targets and estimation of their radar parameter estimation such as delay, Doppler and angle-of-arrival (AoA) using OTFS modulation.

## Table of contents

|       |   |    |
|-------|---|----|
| 1     | CHAPTER 1.....  | 8  |
| 1.1   | Introduction:.....  | 8  |
| 2     | CHAPTER 2.....  | 9  |
| 2.1   | OTFS: A New Generation of Modulation:.....                        | 9  |
| 2.2   | Need for new Waveform: .....                                      | 9  |
| 2.3   | OFDM VS OTFS: .....   | 10 |
| 3     | CHAPTER 3.....  | 11 |
| 3.1   | OTFS Principles: .....  | 11 |
| 3.2   | OTFS Modulation scheme.....                                       | 13 |
| 4     | CHAPTER 4.....  | 16 |
| 4.1   | OTFS Input Output relation:.....                                  | 16 |
| 4.2   | Implementation of Hybrid Digital Analog (HDA) Beam forming: ..... | 17 |
| 4.2.1 | Beam forming Output:.....   | 18 |
| 4.3   | Implementation of RADAR equation.....                             | 20 |
| 5     | CHAPTER 5.....  | 21 |
| 5.1   | System Parameter calculation: .....                               | 21 |
| 6     | Chapter 6.....  | 23 |
| 6.1   | System assumptions: .....   | 23 |
| 6.2   | Simulation results: .....   | 23 |
| 6.2.1 | Single Target detection (N=32): .....                             | 23 |
| 6.2.2 | Multiple target detection (N=32):.....                            | 25 |
| 6.2.3 | Single target detection (N=16):.....                              | 26 |
| 6.2.4 | Multiple target detection (N=16):.....                            | 28 |
| 6.2.5 | Target Angle of Arrival (AOA): .....                              | 29 |
| 7     | CHAPTER 7.....  | 30 |
| 7.1   | Conclusion: .....   | 30 |

|     |                    |    |
|-----|--------------------|----|
| 7.2 | References:.....   | 30 |
| 8   | APPENDIX A .....   | 32 |
| 8.1 | MATLAB CODE: ..... | 32 |

## List of figures

|  |    |
|--|----|
| Figure 1 Basic OTFS Modulation Block Diagram: Transmitter and Receiver ..... | 10 |
| Figure 2 Complementarity of time and frequency representations .....         | 12 |
| Figure 3 Delay-Doppler modulation scheme .....                               | 13 |
| Figure 4 OTFS Transmission and Reception .....                               | 15 |
| Figure 5 Block diagram of OTFS modulation and demodulation .....             | 15 |
| Figure 6 Single target detection and Multi target detection .....            | 17 |
| Figure 7. Beam forming Output: target at 70 deg .....                        | 19 |
| Figure 8. Target simulation and Detection with OTFS .....                    | 22 |
| Figure 9 Single target detection (N=32) .....                                | 23 |
| Figure 10 Target detection at range 140m .....                               | 24 |
| Figure 11 Target detection at Doppler bin 16 .....                           | 24 |
| Figure 12 multiple target detection (N=32) .....                             | 25 |
| Figure 13 Target detection at range 100m, 220m and 350m .....                | 25 |
| Figure 14 Target detection at Doppler bin 9, 16 and 21 .....                 | 26 |
| Figure 15 Single target detection (N=16) .....                               | 26 |
| Figure 16 Target detection at range 140m .....                               | 27 |
| Figure 17 Target detection at Doppler bin 8 .....                            | 27 |
| Figure 18 Multiple target detection (N=16) .....                             | 28 |
| Figure 19 Multiple target detection range 100m, 220m, 350m .....             | 28 |
| Figure 20 Multiple target detection Doppler bin at 5,8,11. ....              | 29 |
| Figure 21 Target detection at AOA 90 deg .....                               | 29 |

## **List of Tables**

|  |    |
|--|----|
| Table 1 System parameters.....             | 21 |
| Table 2 Calculated System Parameters ..... | 22 |



# MIMO Radar with OTFS Modulation

## 1 CHAPTER 1

### 1.1 Introduction:

High mobility use case family such as Mobile services in vehicles, high-speed trains, and even aircraft a growing demand and technologically challenging one [3]. The currently used waveforms fail to perform well in high mobility scenarios where the Doppler shifts witnessed are quite high (e.g., several kHz of Doppler) [3]. Orthogonal time–frequency space (OTFS) is a recently proposed radio access technology waveform suited very well for high-mobility environments. Multiple Doppler introduces ICI in received signal, OFDM fails to equalize multiple Doppler which affects process of detection. MIMO – OTFS is having better performance over MIMO–OFDM in high Doppler environment [3]. OTFS uses delay Doppler domain for channel representation as well as multiplexing of information symbols. OTFS basis functions have strong resilience to delay Doppler shifts impaired by the channel [1]. In this project, I will demonstrate that radar target (moving vehicle) detection and parameter estimation with a mono- static MIMO Radar using MATLAB based simulation. This simulation consists of channel, noise, radar equation modelling and range detection algorithm using matched filtering (pulse compression). The Project report is organized as follows, In Chapter 2 contains introduction of OTFS, performance of OTFS over OFDM, Chapter 3 explain about OTFS principles and modulation schemes, In chapter 4 exploits implementation of OTFS Modulation, Hybrid digital analog beam forming and radar equation, chapter 5 discusses the system parameter calculation from given parameter and simulation results are explained in chapter 6. Chapter 7 concludes the project.

## 2 CHAPTER 2

### 2.1 OTFS: A New Generation of Modulation:

The RADCOM (tasks of Radar and communication) systems are widely used in many areas such as commercial, civilian, aeronautical and military areas. But Radcom systems has the limitations of support, emerging applications such as intelligent automotive systems with high mobility and dense traffic environment requiring very high data rate, ultra reliability, and ultra-low latency communications [4]. To mitigate these limitations, it is required to develop new waveform to perform both functions of radar and communication. Orthogonal time–frequency space (OTFS) modulation, proposed by Hadani in WCNC'2017 [7], is a multiplexing scheme suited well for Time, frequency selective channels. This two dimensional (2D) modulation scheme uses an approach where *multiplexing of information symbols happens in the delay–Doppler domain* [7-11]. This is different from conventional modulation approaches (e.g., OFDM), where multiplexing is done in the time–frequency domain. The delay–Doppler domain provides as an alternative representation of a time-varying channel geometry due to moving objects in the scene.

### 2.2 Need for new Waveform:

The traditional OFDM technique suffers performance degradation in the presence of time and frequency selectivity [5] [6]. Under non-trivial dynamic channel conditions like vehicle-to-vehicle and high-speed rail, where adaptation becomes unrealistic, rendering OFDM narrowband waveforms strictly suboptimal. OTFS is a modulation scheme that carries information QAM symbols over a new class of waveforms which are spread over both time and frequency while remaining roughly orthogonal to each other under general delay-Doppler channel impairments. The key characteristic of the OTFS waveforms is related

to their optimal manner of interaction with the wireless reflectors. This interaction induces a simple and symmetric coupling between the channel response and the information carrying QAM symbols, thus facilitating the design of transmitter and receiver structures with optimal performance complexity trade-off. In summary, OTFS combines the reliability and robustness of spread spectrum with the high spectral efficiency and low complexity of narrowband transmission.

### 2.3 OFDM VS OTFS:

Wireless channels in high-mobility scenarios are time and frequency selective, where multipath effects result in inter-symbol interference (due to frequency selectivity) and high Doppler shifts make the channel highly time selective [12]. The currently used waveforms fail to perform well in high-mobility scenarios where the Doppler shifts encountered are high (e.g., several kHz of Doppler). For example, orthogonal frequency division multiplexing (OFDM)-based systems, while resilient to inter-symbol interference (ISI), suffer from performance degradation due to inter-carrier interference (ICI) caused by high Doppler shifts. Pulse shaping is one approach to jointly mitigate ISI and ICI in OFDM systems. This approach uses time–frequency domain and optimal pulse shapes for the waveform design. However, pulse shaping is not very effective in handling time selectivity in high-mobility channels.

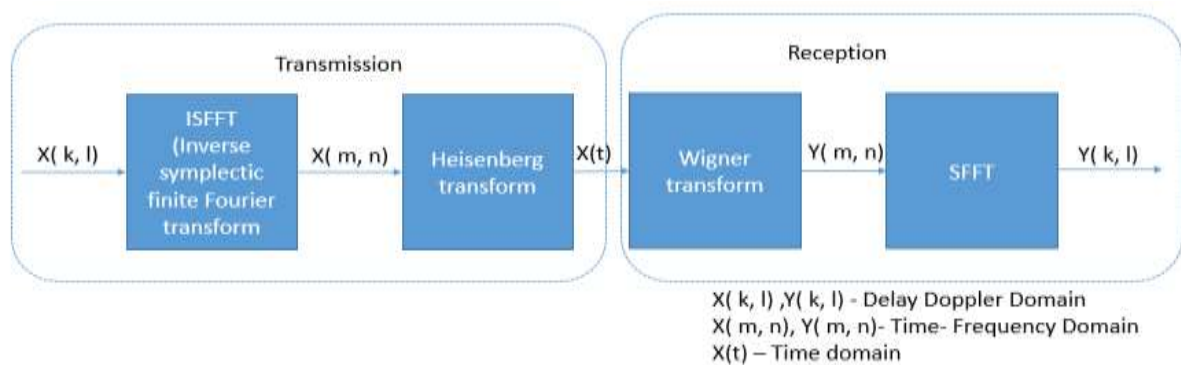


Figure 1 OTFS: Transmitter and Receiver

OTFS has been shown to achieve significant performance gains compared to OFDM in high-Doppler channels with vehicular speeds of 500 km/h in 4 GHz band and 40 km/h in 28 GHz band [7], [10], [11]. OTFS modulation can be implemented using the existing multicarrier modulation schemes (such as OFDM) using additional pre- and post-processing 2D transforms.

### 3 CHAPTER 3

#### 3.1 OTFS Principles:

The delay-Doppler representation generalizes time and frequency representations, generally a combination of TDM (Time Division Multiplexing, or single carrier multiplexing) where QAM symbols are multiplexed over consecutive time slots and FDM (Frequency Division Multiplexing, or multi-carrier multiplexing) where QAM symbols are multiplexed over consecutive frequency carriers[1].

The OTFS waveforms does simple symmetric coupling between the channel and the information carrying QAM symbols. The symmetry manifests itself through three fundamental properties [1]:

- I. Invariance
- II. Separability
- III. Orthogonality

**Invariance** means that the all symbols experience the same channel coupling pattern. **Separability** (hardening) means that all the diversity paths are separated from one another and each QAM symbol experiences all the diversity paths of the channel. Finally, **orthogonality** means that the coupling is localized, which implies that the QAM symbols remain orthogonal to each another at the receiver.

OTFS architected as a multicarrier modulation scheme by means of a two-dimensional (symplectic) Fourier transform between a grid in the delay- Doppler plane and a grid in the reciprocal time-frequency plane. The Fourier relation gives rise to a family of orthogonal 2D basis functions on the time-frequency grid where each of these basis functions can be viewed as a code word that spreads over multiple tones and multiple multicarrier symbols. The time and frequency representations are complementary to one another. Heisenberg uncertainty principle states that a signal cannot be simultaneously localized to any desired degree in time and in frequency. Specifically, if a signal is localized in time then it is non-localized in frequency and vice versa as shown in Figure 2. There exists signals which can be simultaneously localized to any desired degree both in time

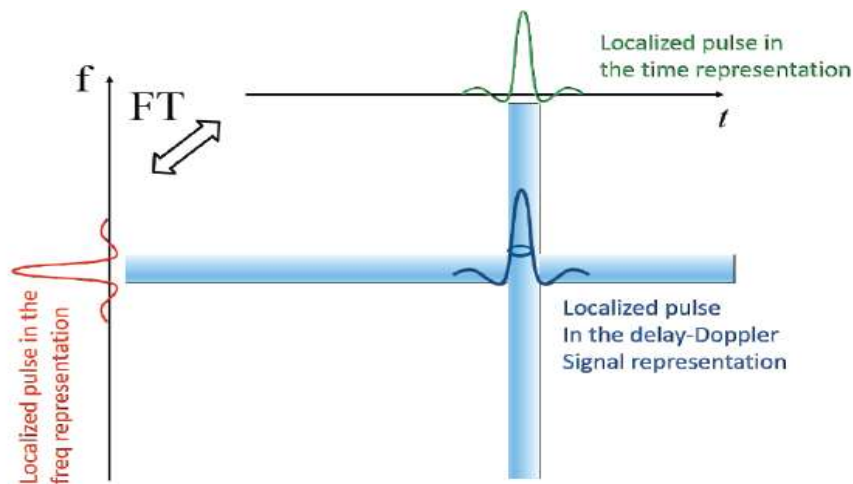


Figure 2 Complementarity of time and frequency representations

and in frequency, a property which perfectly matches both delay-Doppler Radar multi-target detection and for wireless communication. These special signals are associated with localized pulses in a representation called the delay- Doppler representation. The Delay, Doppler represented by two variables  $\tau, \nu$  where the first variable is called delay and the second variable is called Doppler.

### 3.2 OTFS Modulation scheme

The channel-symbol coupling depends both the channel and the modulation carrier waveforms [1]. Every modulation scheme gives output of unique coupling pattern. There are two modulation scheme TDM and FDM in which, the first scheme multiplexes QAM symbols over localized pulses in the time representation and it is called TDM (Time Division Multiplexing). The second scheme multiplexes QAM symbols over localized pulses in the frequency representation (and transmits them using the Fourier transform) and it is called FDM (Frequency Division Multiplexing) [1].

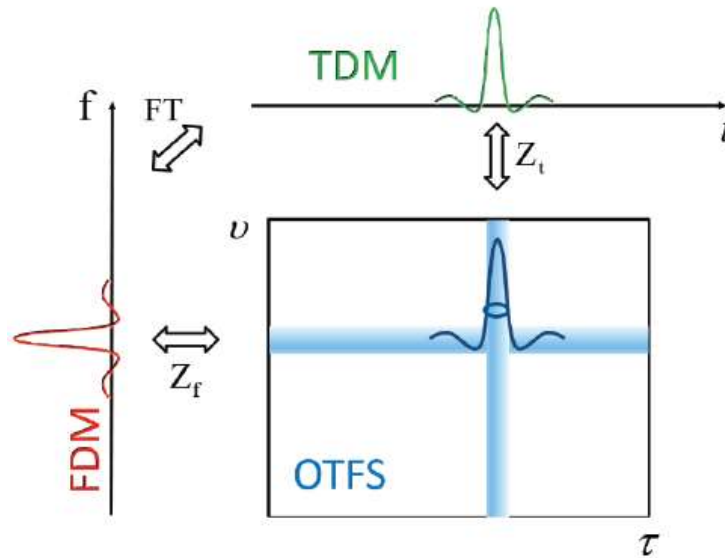


Figure 3 Delay-Doppler modulation scheme

Zak transforms ( $Z_t, Z_f$ ) converts the TDM and FDM carrier pulses to the delay-Doppler representation. Converting the TDM pulse reveals a quasi-periodic function that is localized in delay but non localized in Doppler. Converting the FDM pulse reveals a quasi-periodic signal that is localized in Doppler but non localized in delay. The polarized non-symmetric delay-Doppler representation of the TDM and FDM pulses suggests a superior modulation based on symmetrically localized signals in the delay-Doppler representation called OTFS

modulation, as shown in Figure 3 [1]. The OTFS modulation smoothly interpolates between time and frequency division multiplexing.

There are two method to implement OTFS modulation and demodulation are discussed below.

**Method 1:** The Delay Doppler domain data is transmitted using two steps first converted into time- frequency domain by ISFFT (Inverse symplectic finite Fourier transform) and time- frequency data is converted into time domain data by Heisenberg transform. The received signal is converted into time frequency domain using inverse Heisenberg transform (also Wigner transform) and resulting time-frequency data is transformed into delay Doppler domain using SFFT ( symplectic finite Fourier transform). (Refer Fig 1)

Time frequency input-output relation

$$Y[n, m] = H[n, m]X[n, m]$$

Where,

$$H[n, m] = \sum_{k=0}^{N-1} \sum_{l=0}^{M-1} h[k, l] e^{j2\pi(\frac{nk}{N} - \frac{ml}{M})}$$

ISFFT

$$X[n, m] = \frac{1}{\sqrt{NM}} \sum_{k=0}^{N-1} \sum_{l=0}^{M-1} X[k, l] e^{j2\pi(\frac{nk}{N} - \frac{ml}{M})}$$

SFFT

$$y[k, l] = \frac{1}{\sqrt{NM}} \sum_{n=0}^{N-1} \sum_{m=0}^{M-1} Y[n, m] e^{j2\pi(\frac{nk}{N} - \frac{ml}{M})}$$

**Method 2:** The below block diagram (Fig 4 shows implementation OTFS using ZAK transformation). OTFS transmitter implements inverse ZAK transform i.e. taking IFFT over row wise in delay Doppler domain to convert them into time domain (2D $\rightarrow$ 1D). OTFS receiver implements ZAK transform i.e. taking FFT

over row wise in time domain to convert them into delay Doppler domain (1D--  
→2D)

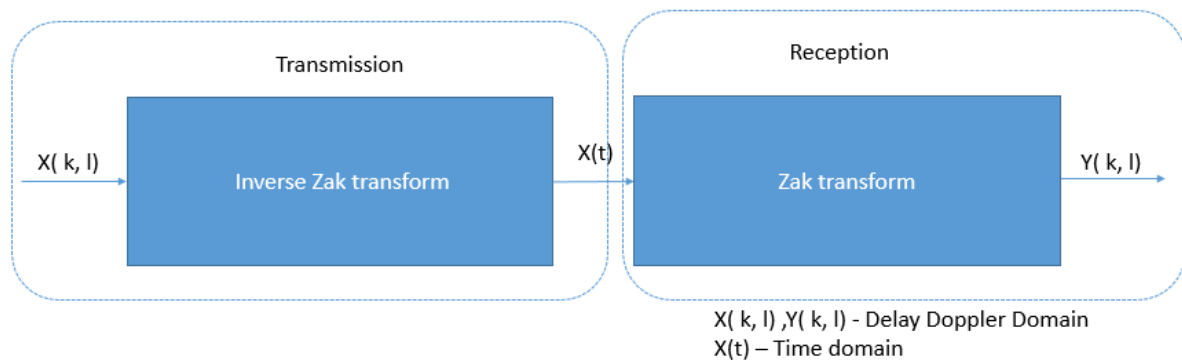


Figure 4 OTFS Transmission and Reception

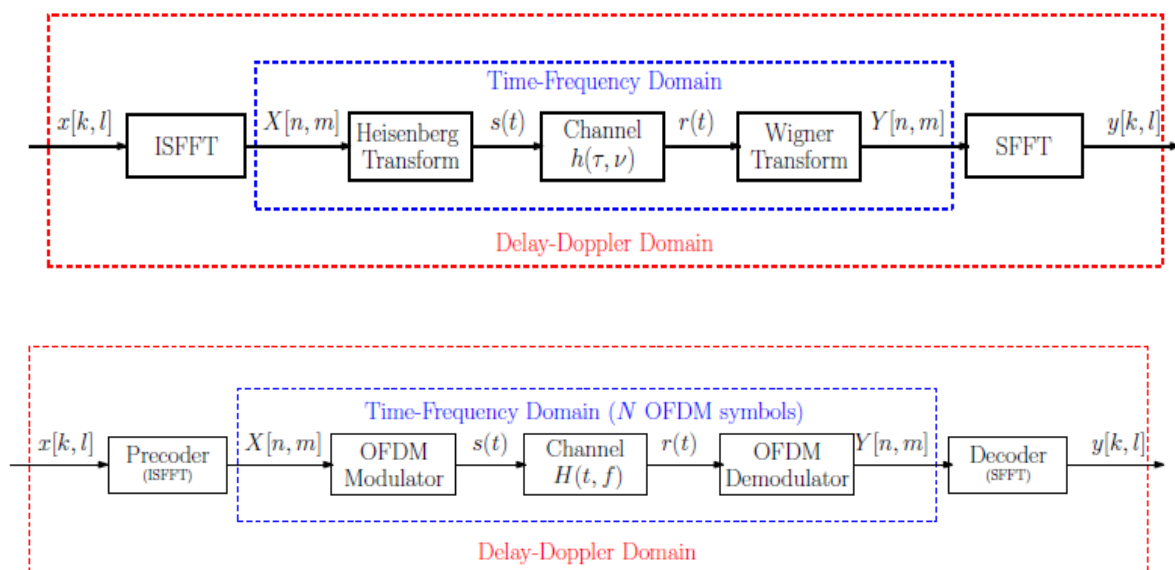


Figure 5 Block diagram of OTFS modulation and demodulation

Time - frequency domain is similar to an OFDM system with N symbols in a  
Frame (Pulse-Shaped OFDM)

- OTFS is compatible with LTE system (Refer Fig 5)
- OTFS can be easily implemented by applying a pre coding and decoding blocks on N consecutive OFDM symbols



## 4 CHAPTER 4

### 4.1 OTFS Input Output relation:

We consider OTFS with  $M$  subcarriers of bandwidth  $\Delta f$  is calculated from bandwidth is given by  $B=M \Delta f$ . We let  $T$  denote the symbol time is calculated from  $T \Delta f = 1$ , yielding the OTFS frame duration of  $NT$ , with  $N$  number of symbols in time [2]. Let denote  $N_s$  the number of data streams to be sent per time-frequency domain such that  $N_s = 1$  corresponds to the multicasting of a single data stream and  $N_s \leq N_{rf}$  (No of RF chain) corresponds to the broadcasting of individual data streams.  $N_s$ -dimensional data symbols  $\{X_{k,l}\}$ , for  $k=0, \dots, N-1$ ,  $l=0, \dots, M-1$ , belonging to any constellation, are arranged in an  $N \times M$  two-dimensional grid referred to as the Doppler-delay domain, The Tx first applies the inverse symplectic finite Fourier transform (ISFFT) to convert data symbols  $\{X_{k,l}\}$ , into a  $N_s \times 1$  block  $\{X[n, m]\}$  in the time- frequency domain [2].

$$X[n, m] = \sum_{k=0}^{N-1} \sum_{l=0}^{M-1} X_{k,l} e^{j2\pi \left( \frac{nk}{N} - \frac{ml}{M} \right)}$$

for  $n=0, \dots, N-1$ ,  $m=0, \dots, M-1$  satisfying the average power constraint. After assigning  $N_s$  streams to  $N_{rf}$  RF chains through a mapping matrix  $V \in \mathbb{C}^{N_{rf} \times N_s}$  the Tx generates the  $N_{rf}$ -dimensional continuous-time signal

$$s(t) = V \sum_{n=0}^{N-1} \sum_{m=0}^{M-1} X[n, m] e^{j2\pi m \Delta f(t)}$$

For any HDA architecture, the transmitter applies the hybrid BF matrix denoted by  $F \in \mathbb{C}^{N_a \times N_{rf}}$ , receiver projection matrix denoted by  $U \in \mathbb{C}^{N_{rf} \times N_a}$

By transmitting the signal over the channel, the Nrf - dimensional continuous-time received signal is given by

$$r(t) = \sum_{p=0}^{P-1} h_p U_b(\phi_p) a^H(\phi_p) F s(t - \tau_p) e^{i2\pi v_p t}$$

The received signal  $y[n, m]$  (Weigner transform of  $r(t)$ ) in the delay-Doppler domain is obtained by the application of the symplectic finite Fourier transform (SFFT)

$$y[k, l] = \sum_{n,m} \frac{y[n, m]}{NM} e^{j2\pi(\frac{ml}{M} - \frac{nk}{N})}$$

## 4.2 Implementation of Hybrid Digital Analog (HDA) Beam forming:

The first scenario considers a wide angular beam (Figure 6) in order to perform the target detection and parameter estimation [2]. The second scenario considers multiple target detection and estimating their parameters. Under this setup, we propose a Matched filter scheme combined with hybrid beam forming to jointly perform target detection and parameter estimation.

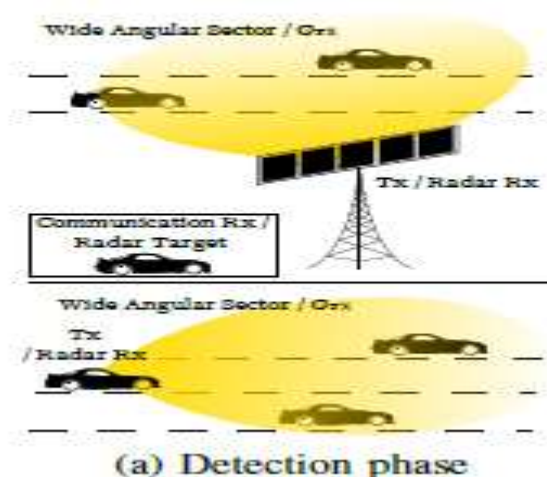


Figure 6 Single target detection and Multi target detection.

### 4.2.1 Beam forming Output:

**Physical model** [2]. : system operates over a channel bandwidth  $B$  at the carrier frequency  $f_c$ . It is assumed that transmitter installed with a mono-static MIMO radar with  $N_a$  antennas and  $N_{rf}$  RF chains, operating in full-duplex mode. The radar Receiver (which is co-located with the Transmitter) processes the return signal to identify the presence of target within the beam, simultaneously estimating parameters of interest such as range, velocity, and AoA. A point target model is considered into account, such that each target can be represented through its line-of-sight (LoS) path only. By letting  $\phi \in [-\frac{\pi}{2}, \frac{\pi}{2}]$  be the steering angle, by considering an antenna array with  $\lambda/2$  spacing ( $\lambda$  is the wavelength), the Tx and Rx arrays are given by  $a(\phi)$  and  $b(\phi)$  respectively, where  $a(\phi) = (a_1(\phi) \dots a_{N_a}(\phi))^T$  denotes the uniform linear array response vector of the radar Rx with

$$a_n(\phi) = e^{j(n-1)\pi\sin(\phi)}, n = 1 \dots N_a$$

And  $b(\phi) = a_n(\phi)$  under the mono-static radar assumption, i.e., same angle at radar Transmitter and Receiver, vectors  $a$  and  $b$  result to be equal. The channel is modelled as a P-tap time-frequency selective channel of dimension  $N_a \times N_a$  given by

$$H(t, \tau) = \sum_{p=0}^{P-1} h_p U b(\phi_p) a^H(\phi_p) \delta(t - \tau_p) e^{i2\pi v_p t}$$

Where  $P$  is the number of targets,  $h_p$  is a complex channel gain including the path loss.

Round-trip Doppler shift  $V_p = \frac{2f_c v_p}{c}$

Round-trip delay  $\tau_p = \frac{2r_p}{c}$

$\phi_p$  denotes the AoA, each corresponding to the  $p^{\text{th}}$  target, respectively

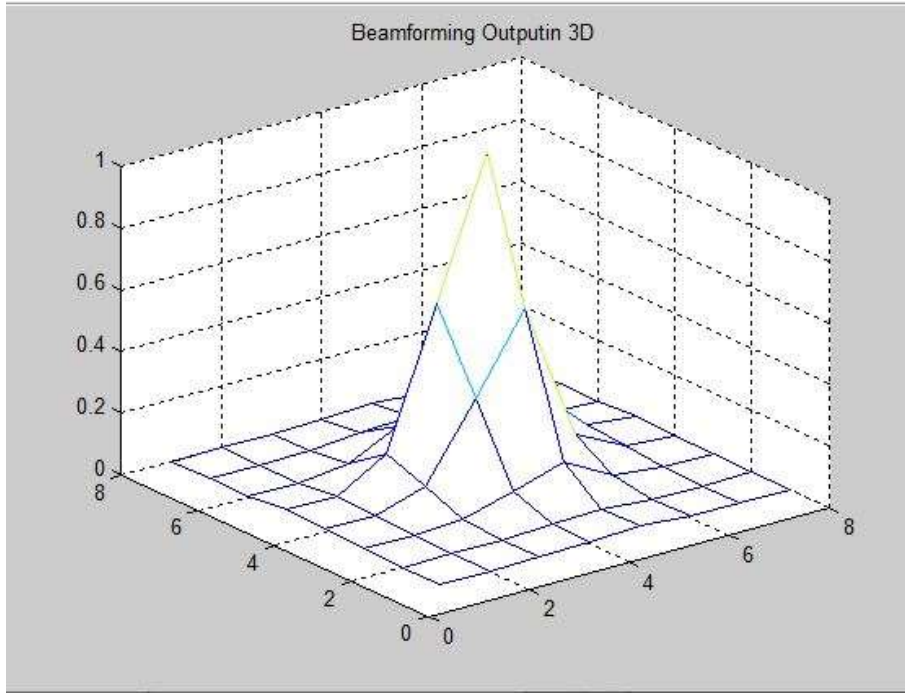


Figure 7. Beam forming Output: target at 70 deg

**Detection Phase [2].** : The design of BF matrix  $F$  at the radar Tx depends on the operating phase. During the detection phase depicted in Fig. 6a, we choose  $F$  for a given angular sector such that both Tx and Rx are aligned towards the same wide angular sector.

We construct  $F \in \mathbb{C}^{N_a \times N_{rf}}$  to cover a wide angular sector  $[-\theta, \theta]$  as follows. By representing this angular sector by a discrete set of  $N_{rf}$  angles, denoted by

$$\Theta = \left\{ \pm \left( \frac{\theta}{2N_{rf}} \right) + k\theta/N_{rf} \right\}, \text{ for } k = 0, \dots, \frac{N_{rf}}{2}-1$$

We construct each column of  $F = [f_1, \dots, f_{N_{rf}}]$  as  $f_i = \frac{a(\theta_i)}{|a(\theta_i)|}$   $i = 1, \dots, N_{rf}$

$$a_n(\phi) = e^{j(n-1)\pi \sin(\phi)}, n = 1 \dots N_a$$

$$a(\phi) = (a_1(\phi) \dots a_{N_a}(\phi))^T$$

$$U = F^H, b(\phi)=a_n(\phi)$$

### 4.3 Implementation of RADAR equation

Radar equation has been included in the simulation. In order to calculate received signal from target, radar equation is used as below. The distant targets is relatively very small because received power declines as the fourth power of the range. In order increase the range by two times, we require sixteen times more power than what we have used for the radar.

The Radar Range Equation shows target Properties in terms of radar cross section, Radar Characteristics - e.g. Transmitter Power, Antenna gain, Distance between Target and Radar.

The radar SNR,

$$SNR = \frac{P_{avg} G_{Rx} G_{Tx} \sigma_{rcs} \lambda^2}{4\pi^3 r^4 \sigma_w^2}$$

$G_{Rx}$  – Antenna Gain at RX (dB)

$G_{Tx}$  – Antenna Gain at Tx (dB)

$r$  - Distance between Tx and Rx (m)

$\lambda$  - Wavelength (m)

$\sigma_w^2$  –The variance of the AWGN noise  
with noise power spectral density (PSD)

$P_{avg}$ - Average transmitted power in W

$\sigma$ - Target Radar cross section (m<sup>2</sup>)

The velocity and the range resolution is determined by the system parameters in Table I and given by

$$v_{res} = \frac{BC}{2NMf_c} \text{ m/s}$$

$$r_{res} = \frac{C}{2B} \text{ m}$$

In order to get a reasonable range resolution, e.g.,  $< 1$  [m], a large bandwidth has to be considered. Pulse compression technique allows a radar to utilize a long pulse to achieve large radiated energy, but simultaneously to obtain the range resolution of a short pulse. Since the velocity resolution is directly proportional to  $B$  [2]. , for a fixed  $f_c$ , the only way to obtain lower values (means better resolution) is to increase the block size  $NM$ , leading to a remarkable increase in computational complexity which results more cost. For this reason, we set the system parameters by focusing on a reasonable range resolution (and theoretical maximum range) under a feasible computational complexity. Note that the maximum range could not be achieved if the backscattered power is below the noise floor.

## 5 CHAPTER 5

### 5.1 System Parameter calculation:

System parameters has been calculated from given parameters Table 1. Sub carrier Bandwidth, Velocity Resolution ( $V_{res}$ ), Range Resolution, Doppler frequency, Symbol time, Delay, Maximum velocity and Maximum Range are calculated from given system parameters.

#### System parameters:

|  |                                      |
|--|--------------------------------------|
| $N = 6, 32$                              | $M = 512$                            |
| $F_c = 24.25$ GHz                        | $B = 150$ MHz                        |
| $V_{res} = 440$ Km/h                     | $r_{res} = 1$ m                      |
| $V_{max} = N \cdot V_{res}$              | $R_{max} = M \cdot r_{res}$          |
| $P_{avg} = 40$ mW                        | $\sigma_{rcs} = 1$ m <sup>2</sup>    |
| Noise figure = 3 dB                      | Noise PSD = $2 \times 10^{-21}$ W/Hz |
| Antenna array<br>$N_a = 16, 32, 64, 128$ | Number of channel $N_{rf} = 8$ ;     |

Table 1 System parameters

### Calculated System parameters:

| S. No | System Parameters                          | Value           |
|-------|--|-----------------|
| 1.    | Antenna array $N_a$                        | 16              |
| 2.    | $N$  | 16,32           |
| 3.    | Number of channel $N_{rf}$                 | 8               |
| 4.    | Max target Range                           | $R_{res}.M$     |
| 5.    | Sub carrier BW $\Delta f$<br>(BandWidth/M) | $2.9297e+05Hz$  |
| 6.    | Delay= $1/\Delta f$                        | $3.4133e-06sec$ |
| 7.    | Doppler resolution                         | $Delay(FS)/N$   |
| 8.    | symbol time( Delay/M)                      | $6.6666e-09sec$ |

Table 2 Calculated System Parameters

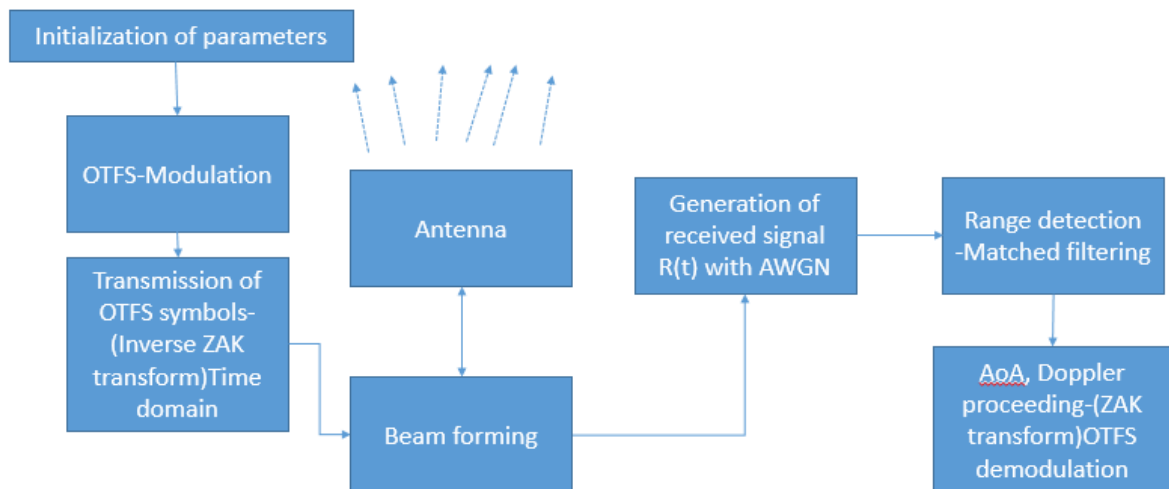


Figure 8. Target simulation and Detection with OTFS

**Note:**  $V_{res} = \text{Band Width} * C / (2 * N * M * f_c)$ ; For  $N=6$ ; It is observed that  $V_{res} = 1087km/h$  and maximum velocity can be achieved  $V_{max}=N. V_{res} = 6552km/h$ . But it is not matching with given system parameters  $V_{res}$  i.e.  $440Km/h$ . So I assumed  $N=16$ ; and  $V_{res}=408Km/h$  which matches given system parameters. For  $N=32$ ,  $V_{res}=203Km/h$ . For  $N=32$  Doppler bin resolution =  $9.1553e+03$  Hz, For  $N=16$  Doppler bin resolution =  $1.8311e+04$  Hz.

## 6 Chapter 6

### 6.1 System assumptions:

- Given the choice of a mmWave communication, we assume a single LoS path between the Tx and the radar target. This is motivated by the fact that any possible scattering component different from the LoS generally brings much lower power, given by additional reflections of the echo signal [2].
- Any backscattered power to the radar Rx is considered as a possible target. The objective is to sense the surrounding environment, and the differentiation between active targets and obstacles is a post-processing decision [2].

### 6.2 Simulation results:

#### 6.2.1 Single Target detection (N=32):

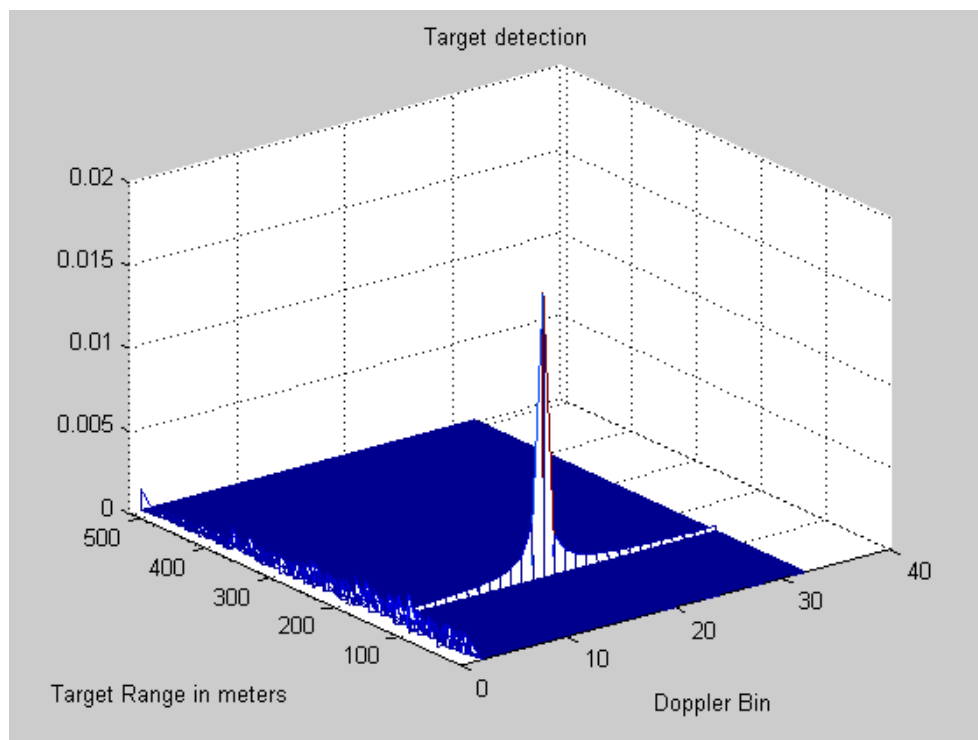


Figure 9 Single target detection (N=32)



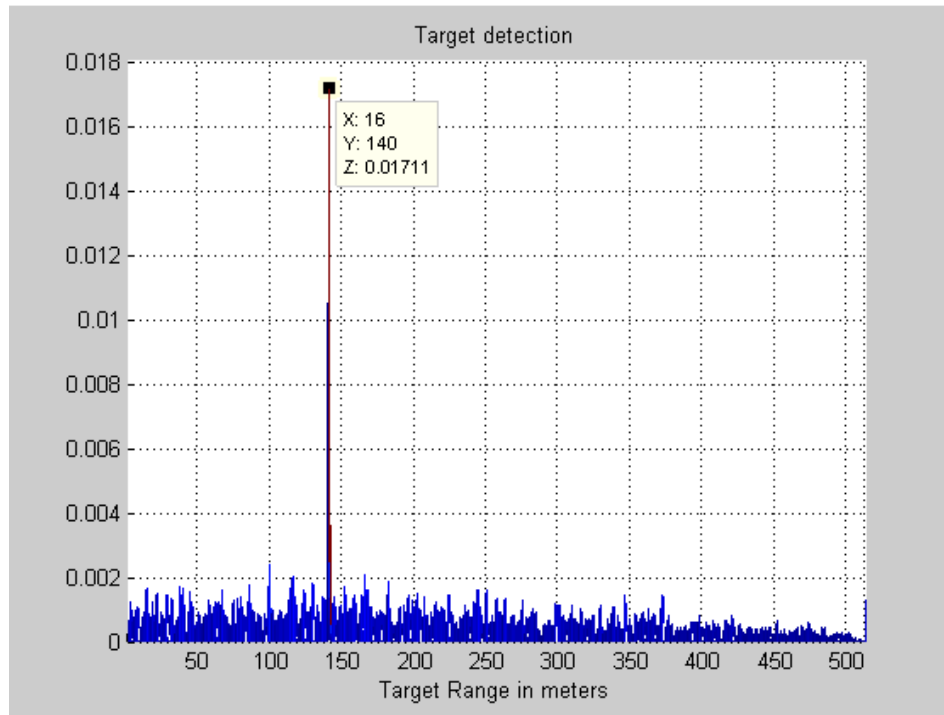


Figure 10 Target detection at range 140m

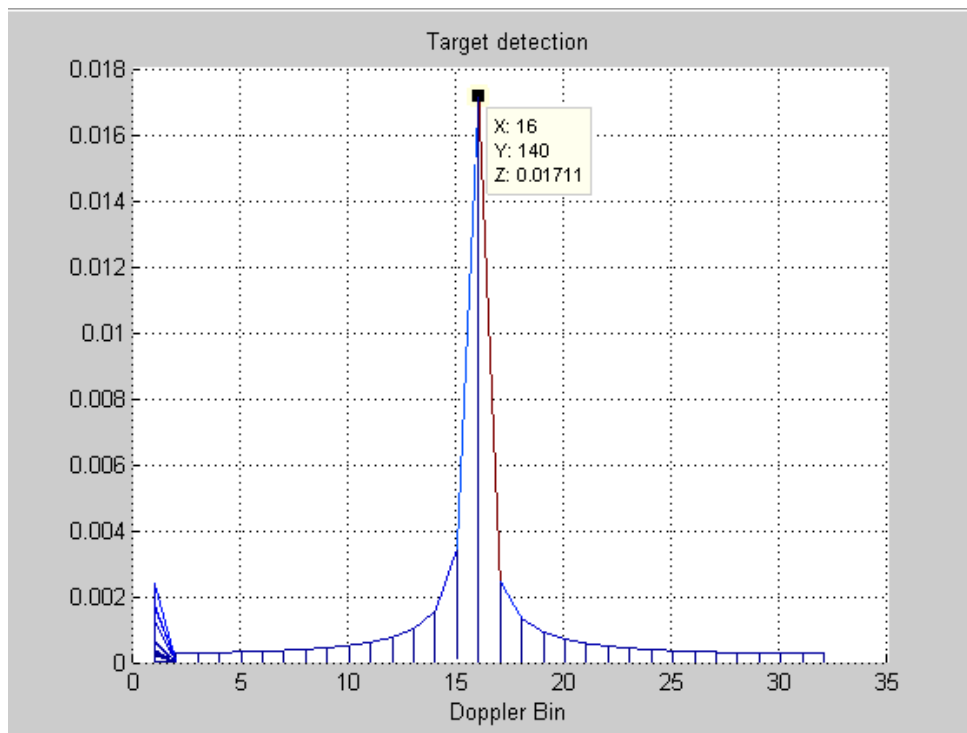


Figure 11 Target detection at Doppler bin 16

| S. No | Injected Doppler frequency (Hz) | Detected Doppler frequency (Hz) |
|-------|---------------------------------|---------------------------------|
| 1     | 1.3580e+05                      | 1.4648e+05                      |

### 6.2.2 Multiple target detection (N=32):

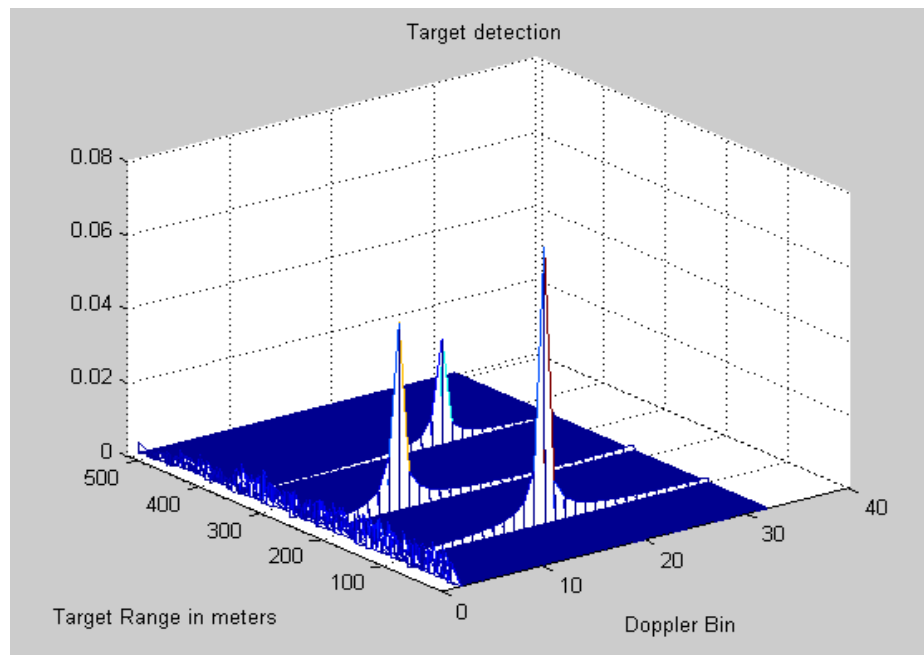


Figure 12 multiple target detection (N=32)

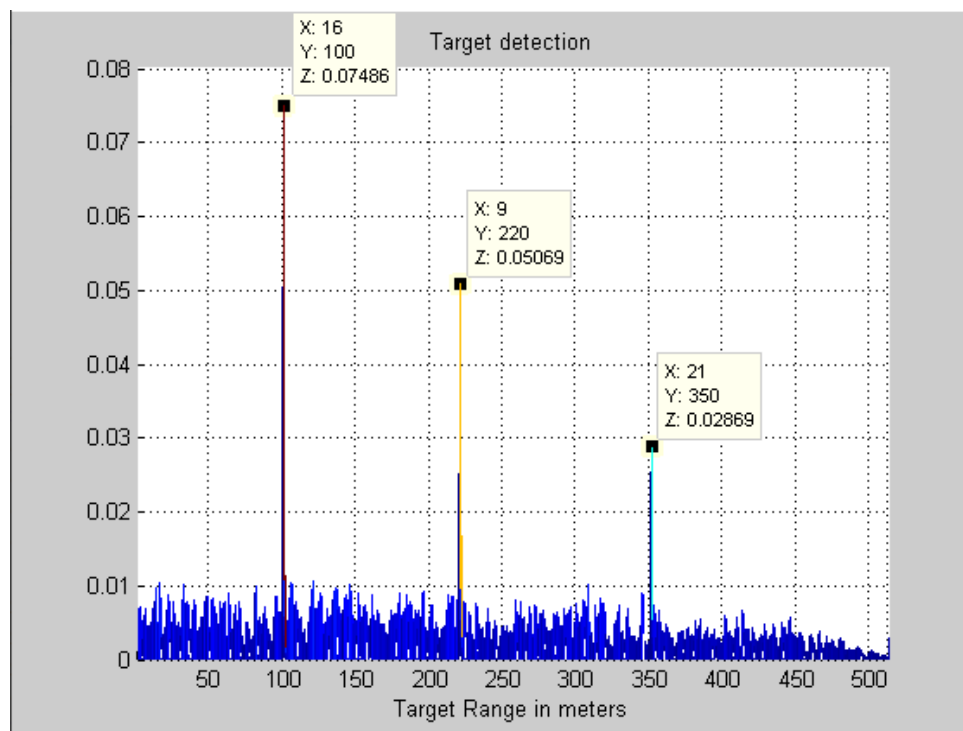


Figure 13 Target detection at range 100m, 220m and 350m

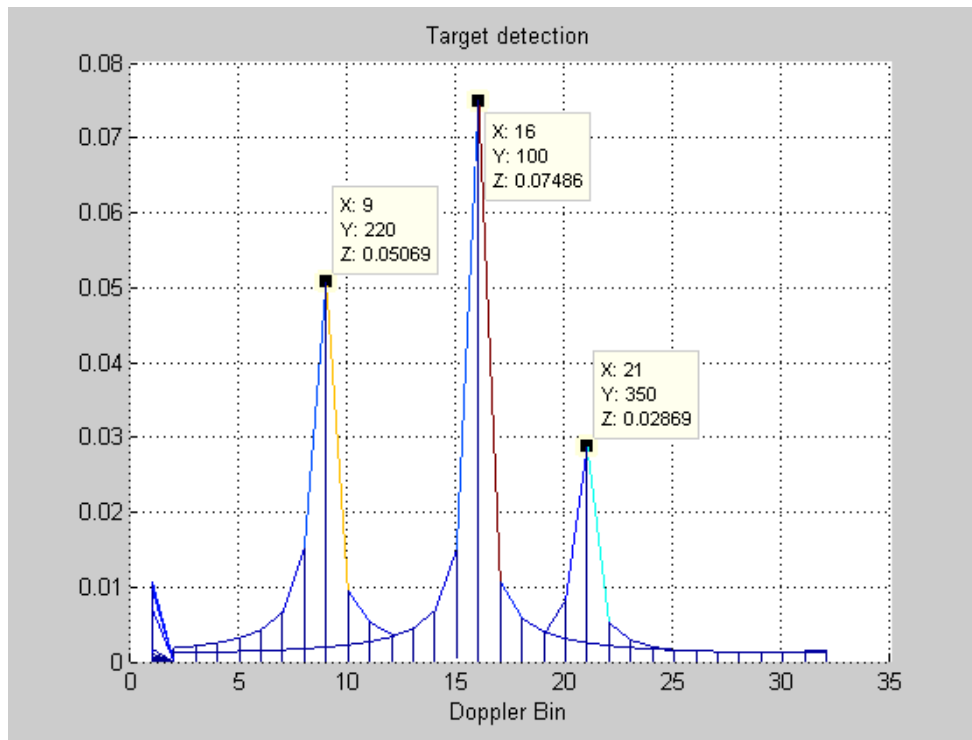


Figure 14 Target detection at Doppler bin 9, 16 and 21

| S. No | Injected Doppler frequency (Hz) | Detected Doppler frequency (Hz) |
|-------|---------------------------------|---------------------------------|
| 2     | 1.3580e+05                      | 1.4648e+05                      |
| 3     | 7.113e+04                       | 8.2397e+04                      |
| 4     | 1.8107e+05                      | 1.9226e+05                      |

### 6.2.3 Single target detection (N=16):

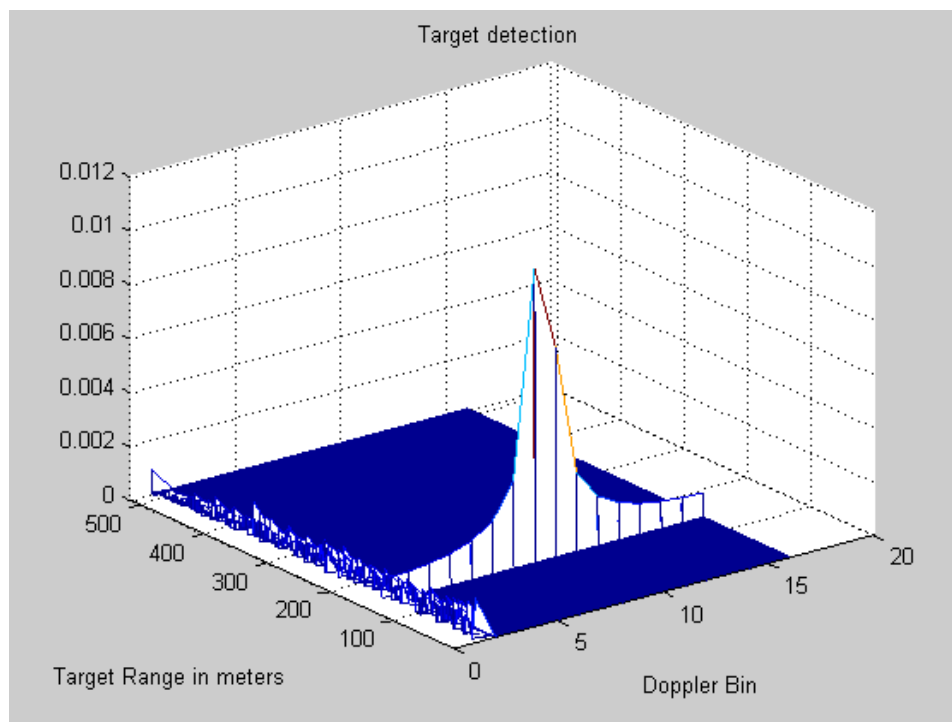


Figure 15 Single target detection (N=16)

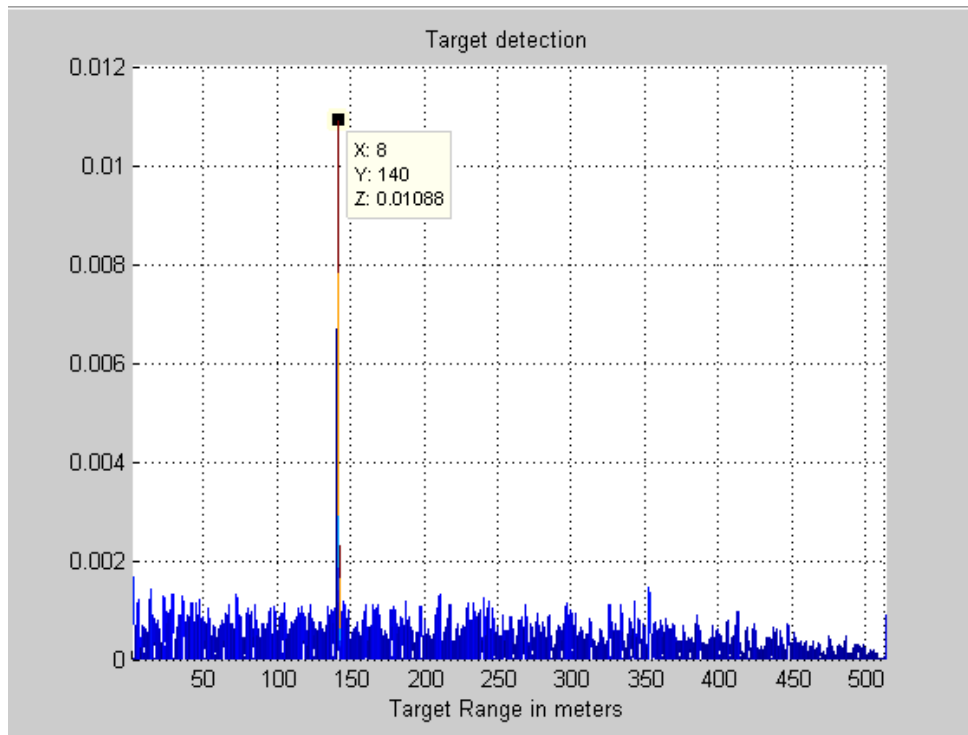


Figure 16 Target detection at range 140m

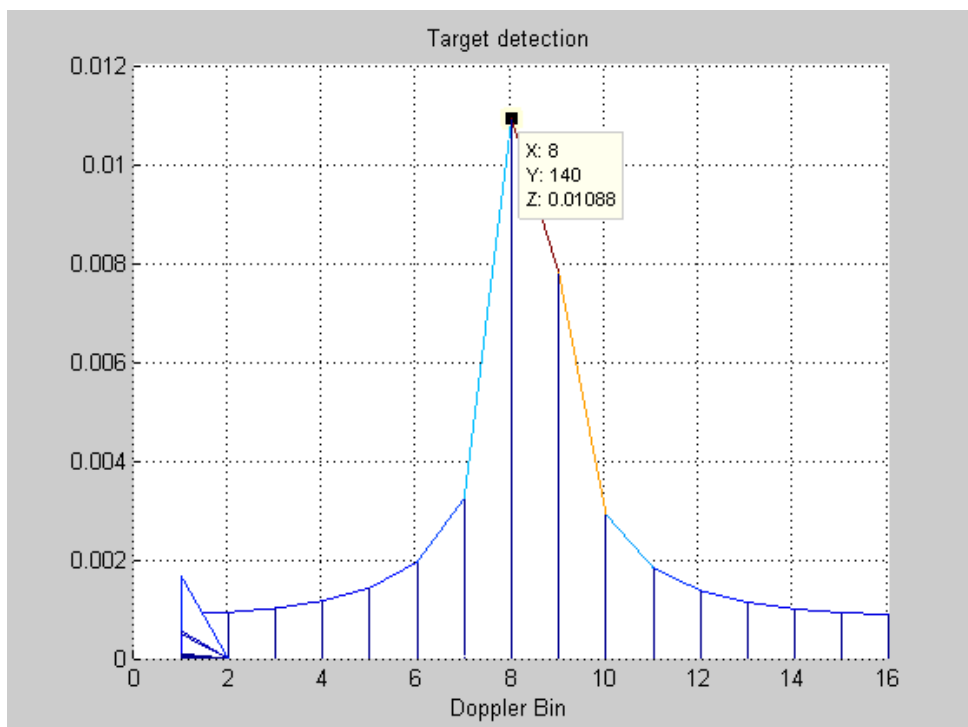


Figure 17 Target detection at Doppler bin 8

| S. No | Injected Doppler frequency (Hz) | Detected Doppler frequency (Hz) |
|-------|---------------------------------|---------------------------------|
| 5     | 1.3580e+05                      | 1.4648e+05                      |

#### 6.2.4 Multiple target detection (N=16):

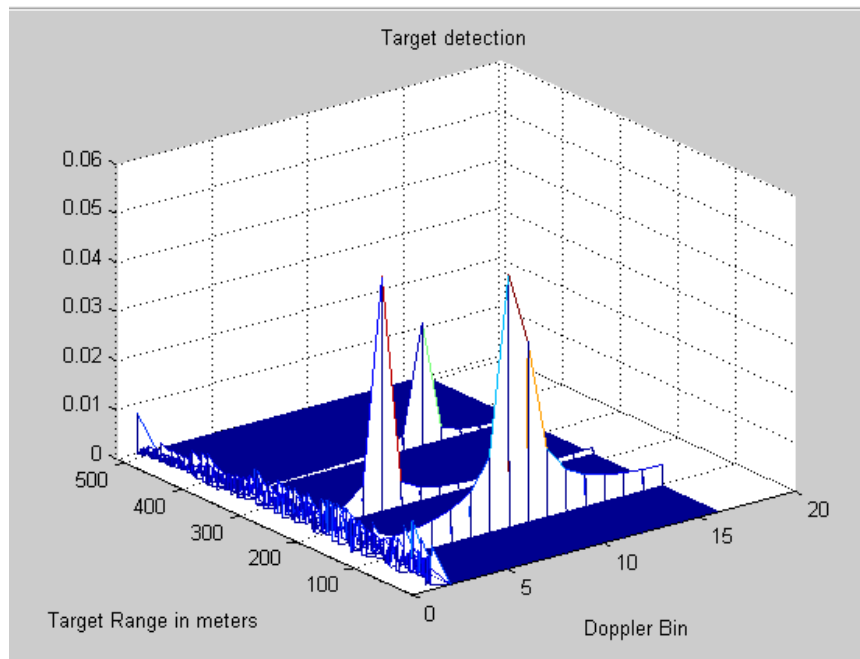


Figure 18 Multiple target detection (N=16)

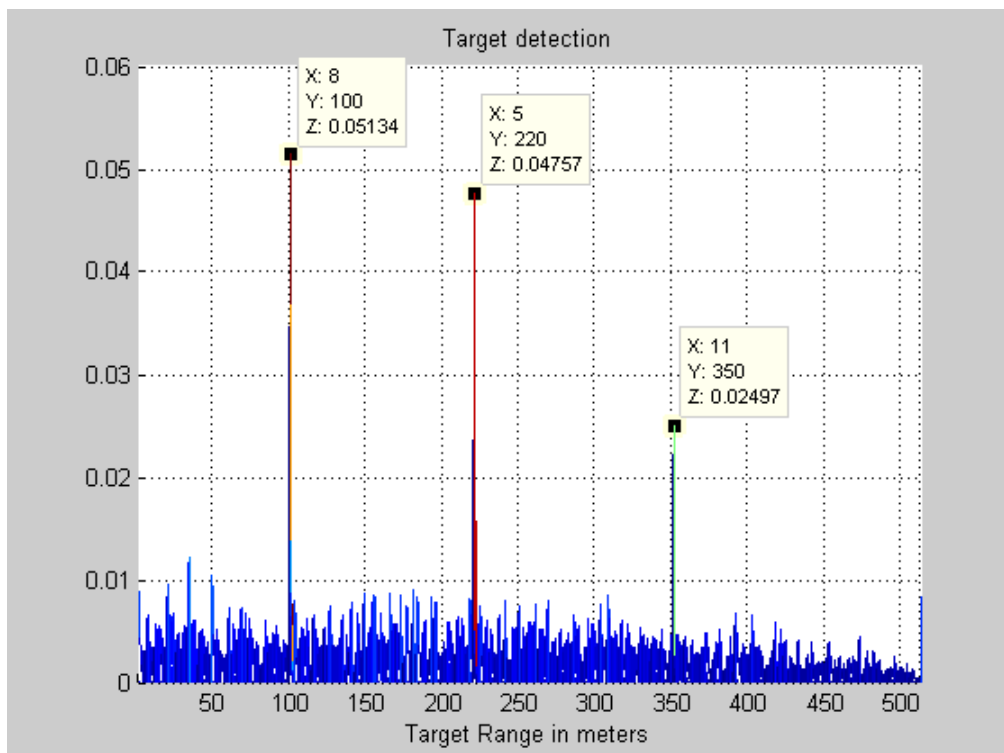


Figure 19 Multiple target detection range 100m, 220m, 350m

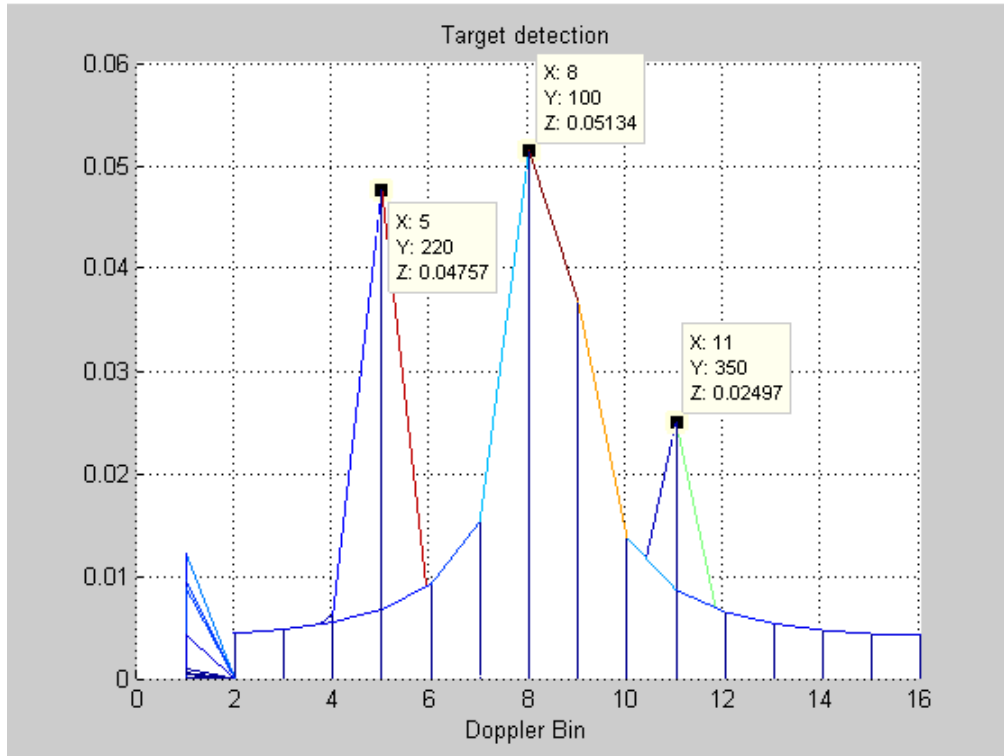


Figure 20 Multiple target detection Doppler bin at 5,8,11.

| S. No | Injected Doppler frequency (Hz) | Detected Doppler frequency (Hz) |
|-------|---------------------------------|---------------------------------|
| 1.    | 1.3580e+05                      | 1.4648e+05                      |
| 2.    | 7.113e+04                       | 9.1553e+04                      |
| 3.    | 1.8107e+05                      | 2.0142e+05                      |

### 6.2.5 Target Angle of Arrival (AOA):

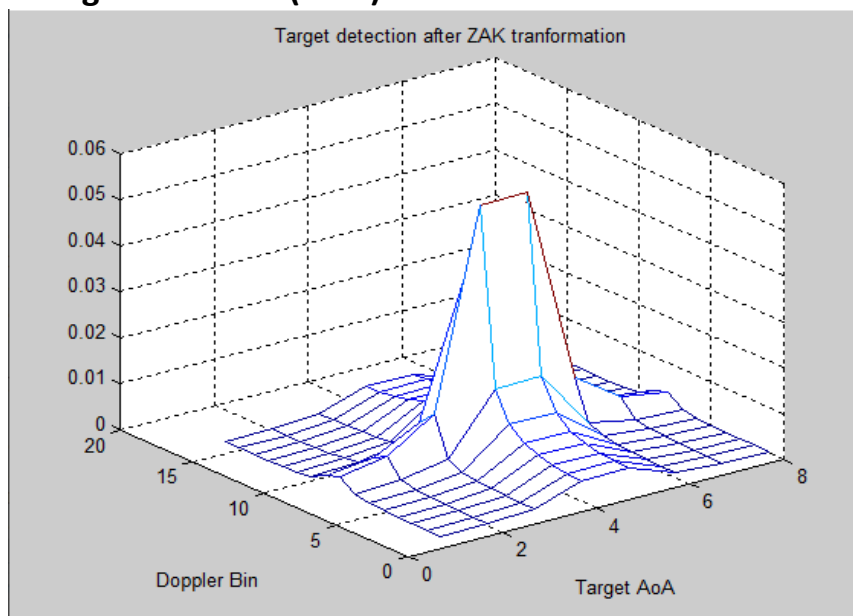


Figure 21 Target detection at AOA 90 deg

## 7 CHAPTER 7

### 7.1 Conclusion:

In this project, I have simulated MIMO mono-static radar based target generation with different Doppler, range and AOA and target detection, radar parameters estimation i.e., range, velocity, and AoA using OTFS modulation and demodulation. And I have implemented modules like Matched filtering algorithm, Hybrid beam forming algorithm and radar equation modules in target detection and parameter estimation process. The basics of OTFS and performance of OTFS have been explained in detail and Simulation results demonstrated that the Radar functionality can be established and radar parameter can be estimated using OTFS modulation. Implementation of communicating message to the moving vehicles from another vehicle, tracking performance of the MIMO Radar, improvement of range and velocity resolution are left as a future work.

### 7.2 References:

1. Hadani R, Monk A (2018) OTFS: a new generation of modulation addressing the challenges of 5G. arXiv :1802.02623 ([cs.IT] 7 Feb 2018)
2. Lorenzo Gaudio, Mari Kobayashi, Giuseppe Caire<sup>3</sup>, Giulio Colavolpe Hybrid Digital-Analog Beamforming and MIMO Radar with OTFS Modulation arXiv:2009.08785v1 [eess.SP] 17 Sep 202
3. Ramachandran, M. K., Surabhi, G. D., & Chockalingam, A. (2020, April 1). OTFS: A New Modulation Scheme for High-Mobility Use Cases. *Journal of the Indian Institute of Science*. Springer. <https://doi.org/10.1007/s41745-020-00167-4>
4. Raviteja, P., Phan, K. T., Hong, Y., & Viterbo, E. (2019). Orthogonal time frequency space (OTFS) modulation based radar system. In D. Rabideau (Ed.), *2019 IEEE Radar Conference (RadarConf)* IEEE, Institute of Electrical and Electronics Engineers.

5. K. T. Truong and R. Heath, "Effects of channel aging in massive MIMO systems," *Journal of Communications and Networks*, vol. 15, no. 4, pp. 338-351, Aug 2013.
6. E. Björnson, et al., "Massive MIMO Systems With Non-Ideal Hardware: Energy Efficiency, Estimation, and Capacity Limits," *IEEE Transactions on Information Theory*, vol. 60, no. 11, pp. 7112-7139, Nov 2014.
7. Hadani R, Rakib S, Tsatsanis M, Monk A, Goldsmith AJ, Molisch AF, Calderbank R (2017) Orthogonal time frequency space modulation. In: *Proc. IEEE WCNC'2017*,
8. Hadani R, Rakib S, Kons S, Tsatsanis M, Monk A, Ibars C, Delfeld J, Hebron Y, Goldsmith AJ, Molisch AF, Calderbank R (2018) Orthogonal time frequency space modulation. *arXiv :1808.00519 v1 [cs.IT]* 1 Aug 2018)
9. Monk A, Hadani R, Tsatsanis M, Rakib S (2016) OTFS— orthogonal time frequency space: a novel modulation technique meeting 5G high mobility and massive MIMO challenges. *arXiv :1608.02993 [cs.IT]* 9 Aug 2016)
10. Hadani R, Rakib S, Molisch AF, Ibars C, Monk A, Tsatsanis M, Delfeld J, Goldsmith A, Calderbank R (Jun. 2017) Orthogonal time frequency space (OTFS) modulation for millimeter-wave communications systems. In: *Proc. IEEE MTT-S Intl. Microwave Symp.*, pp 681–683
11. Surabhi GD, Chockalingam A (2019) OTFS modulation with phase noise in mmWave communications. In: *Proc. IEEE VTC'2019-Spring*
12. Jakes WC (1994) *Microwave mobile communications*. IEEE Press, New York



## 8 APPENDIX A

### 8.1 MATLAB CODE:

```
%%%%%%%%%%%%%%%%%%%%%%%%%%%%%%%%%%%%%%%%%%%%%%%%%%%%%%%%%%%%%%%%%%%%%%%%Project%%%%%%%%%%%%%%%%%%%%%%%%%%%%%%%%%%%%%%%%%%%%%%%%%%%%%%%%%%%%%%%%%%%%%%%%
%%%%%%%%%%%%%%%%%%%%%%%%%%%%%%%%%%%%%%%%%%%%%%%%%%%%%%%%%%%%%%%%%%%%%%%%NAME:RAMKUMAR A%%%%%%%%%%%%%%%%%%%%%%%%%%%%%%%%%%%%%%%%%%%%%%%%%%%%%%%%%%%%%%%%%%%%%%%%
%%%%%%%%%%%%%%%%%%%%%%%%%%%%%%%%%%%%%%%%%%%%%%%%%%%%%%%%%%%%%%%%%%%%%%%%Roll No:EE19M013%%%%%%%%%%%%%%%%%%%%%%%%%%%%%%%%%%%%%%%%%%%%%%%%%%%%%%%%%%%%%%%%%%%%%%%%
%%%%%%%%%%%%%%%%%%%%%%%%%%%%%%%%%%%%%%%%%%%%%%%%%%%%%%%%%%%%%%%%%%%%%%%%Project:MIMO-RADAR with OTFS Modulation%%%%%%%%%%%%%%%%%%%%%%%%%%%%%%%%%%%%%%%%%%%%%%%%%%%%%%%%%%%%%%%%%%%%%%%%
%%%%%%%%%%%%%%%%%%%%%%%%%%%%%%%%%%%%%%%%%%%%%%%%%%%%%%%%%%%%%%%%%%%%%%%%Module:RADAR-using OTFS modulation and
demodulation%%%%%%%%%%%%%%%%%%%%%%%%%%%%%%%%%%%%%%%%%%%%%%%%%%%%%%%%%%%%%%%%%%%%%%%%
clear all;
close all;
clc;
%%%%%%%%%%%%%%%%%%%%%%%%%%%%%%%%%%%%%%%%%%%%%%%%%%%%%%%%%%%%%%%%%%%%%%%%System Parameter settings%%%%%%%%%%%%%%%%%%%%%%%%%%%%%%%%%%%%%%%%%%%%%%%%%%%%%%%%%%%%%%%%%%%%%%%%
M=512;N=32; % M-Delay, N-doppler bins
Na=128; % No of antenna elements
Nrf=8; % No of RF chains
Tgt_angle=90;
theta_pi=(Tgt_angle).*pi/180; %% Target angle
vel=[840 440 1120]; %not Exceed max velocity VMAX %%in m/s
tgtRng=[100 220 350]; %%in meters
fc=24.25*1e9; %%Hz
C_constant=3*1e8; %%m/s
Pt = 40*10^-3; %%Transmit power
NF=3; %%Noise Figure in dB
Noise_PSD=2*10^-21; % power spectral density
Rres=1;
RMAX=M*Rres;
BandWidth=150*1e6;
Del_Frq=BandWidth/M;%%FS
FS=Del_Frq;
Delay=1/Del_Frq;% one frame time(total)
```

```

symbol_time=Delay/M;
lamda=C_constant/fc;
RxGain = 50;    %Antenna receive gain  %%mm wave antenna design assumption
TxGain = 50;    %Antenna Transmit gain
rcs=1;
Vres_cal=BandWidth*C_constant/(2*N*M*fc);
VMAX=N*Vres_cal  %%%% maximum velocity calculation
Doppler_res=2*Vres_cal/lamda  %%= FS/N
%%%%%%%%%%%%%%%%%%%%%%%%%%%%%%%%%%%%%%%%%%%%%%%%%%%%%%%%%%%%%%%%%%%%%%%% System      Parameter      settings-end
%%%%%%%%%%%%%%%%%%%%%%%%%%%%%%%%%%%%%%%%%%%%%%%%%%%%%%%%%%%%%%%%%%%%%%%%

                %%% Beam forming %%%

Sector_angle=180;
k=0:1:(Nrf/2)-1;
Angles= (Sector_angle/(2*Nrf))+((k.*Sector_angle)/Nrf);
Angles_out=[ Angles -(fliplr(Angles)) ]*(pi/180);
doppler_effect=2*vel./lamda;
time_target_delay=2*tgtRng./ C_constant;    %%%round trip delay
for jj=1:Nrf
j=1:Na;
F(:,jj)= exp(1i*(j-1)*pi.*sin(Angles_out(jj)));
end

%      j=1:Na;
%      F(:,1)= exp(1i*(j-1)*pi.*sin(theta_pi(1)));
%      F(:,2)= exp(1i*(j-1)*pi.*sin(theta_pi(2)));
U=F';%%%%NrfxNa
                %%%-----%%target angle---%%%%%%%%
j=1:Na;
aa_pi=exp(1i*(j-1)*pi.*sin(theta_pi));
%aa_pi2=exp(1i*(j-1)*pi.*sin((theta_pi(2)))); %%% to add multiple targt angle
bb_pi=aa_pi';

```

```

%bb_pi2=aa_pi2';
%Beam_out=U*bb_pi*aa_pi*F+(U*bb_pi2*aa_pi2*F);
Beam_out=U*bb_pi*aa_pi*F;%(U*bb_pi2*aa_pi2*F);
%ff=10*log10(abs(Beam_out)/max(max(abs(Beam_out))));
figure,mesh(abs(Beam_out)/max(max(abs(Beam_out))));
title('Beamforming Outputin 3D');
x=0:22.5:180-22.5;
figure,plot(x,abs(Beam_out(1,:))/max(abs(Beam_out(1,:))));
title('Beamforming Output');
xlim[-90 90];

%%% Beam forming-end %%%%

%%%Radar equation- target power calculation %%%%
tgtPow = Pt * 10^(0.1*(RxGain + TxGain)) * lamda^2 * rcs ./((4*pi)^3 * tgtRng.^4); %%

%%% target power calculation-end %%%%

%%%%%%%%OTFS Modulation%%%%%%%%

Qam_Symb=[];%%%%%%%%M*N
for kkk=1:Nrf
    Qam_Symb=[];
    for i=1:N
        r_l= randi([0 1],1,M);
        r_q= randi([0 1],1,M);
        r1=(2*r_l)-1;
        r2=(2*r_q)-1;
        x=(r1+(1i*r2))*(1/sqrt(2));
        Qam_Symb=[x Qam_Symb];
    end
    Qam_Symb=reshape(Qam_Symb,M,N);%%%M*N
    %%%inverse Zak transformation%%%
    for i=1:M
        g(i,:)=ifft(Qam_Symb(i,:));
    end
    Tx_out(kkk,:)=reshape(g,1,[]);%%Nrf*Ns

```

```

end

%%%%%%%%%%%%%%%%%%%%%%%%%%%%%%%%%%%%%%%%%%%%%%%%%%%%%%%%%%%%%%%%%%%%%%%%OTFS Modulation-end%%%%%%%%%%%%%%%%%%%%%%%%%%%%%%%%%%%%%%%%%%%%%%%%%%%%%%%%%%%%%%%%%%%%%%%%

pFFT = 2^ceil(log2(N));
Signal = zeros(M,N);
Mr = floor((tgtRng(1))/Rres);
t=(0:N-1)*Delay;
sigma_2=Noise_PSD*BandWidth*10^{.3};
%%%%%%%%%%%%%%%%%%%%%%%%%%%%%%%%%%%%%%%%%%%%%%%%%%%%%%%%%%%%%%%%%%%%%%%%Inverse Zak transformation %%%%%%%%%%%%%%%%%%%%%%%%%%%%%%%%%%%%%%%%%%%%%%%%%%%%%%%%%%%%%%%%%%%%%%%%%

for i=1:M
Qam_sym_ifft(i,:)=ifft(Qam_Symb(i,:));
end

%%%%%%%%%%%%%%%%%%%%%%%%%%%%%%%%%%%%%%%%%%%%%%%%%%%%%%%%%%%%%%%%%%%%%%%%multiple target generation%%%%%%%%%%%%%%%%%%%%%%%%%%%%%%%%%%%%%%%%%%%%%%%%%%%%%%%%%%%%%%%%%%%%%%%%

Qam_sym_ifft_new=[];
for jj=1:N
gg=Qam_sym_ifft(:,N).';
Qam_sym_ifft1 =([zeros(1,tgtRng(1)) gg(1:M-tgtRng(1))]+([zeros(1,tgtRng(2)) gg(1:M-
tgtRng(2))]+([zeros(1,tgtRng(3)) gg(1:M-tgtRng(3))]]));
%Qam_sym_ifft1 =([zeros(1,tgtRng(1)) gg(1:M-tgtRng(1))]]);
Qam_sym_ifft_new=[Qam_sym_ifft_new Qam_sym_ifft1];
end

Rx_out1= repmat(Qam_sym_ifft_new,Nrf,1); %% for Nrf times
Rx_out=(Beam_out*Rx_out1*tgtPow(1))+(sqrt(sigma_2/2)*(randn(Nrf,M*N)+1i*randn(Nrf,
M*N)));%% Beam forming effect and Noise addition
%Rx_out=(Beam_out*Rx_out1);%+(sqrt(sigma_2/2)*(randn(Nrf,M*N)+1i*randn(Nrf,M*N)));
%% Beam forming effect and Noise addition

Qam_sym_ifft_new3=[];
temp3=[];
temp4=[];
temp5=[];
for ff=1:Nrf
Qam_sym_ifft_new=reshape(Rx_out(ff,:),M,N);
Qam_sym_ifft_new1=[];

```

```

for jj=1:N
    gg=Qam_sym_ifft(:,N).';
    [acor,lag]=xcorr(Qam_sym_ifft_new(:,N),gg);%/sum(abs(Z(i+(N/2):N+i-1)).^2);
    [~,l] = max(abs(acor));
    timeDiff = lag(l);
    xx=[acor(513:1023)' acor(512)];
    Qam_sym_ifft_new1=[Qam_sym_ifft_new1 xx'];
end
Qam_sym_ifft_new2=reshape(Qam_sym_ifft_new1,M,N);
Qam_sym_ifft_new2(tgtRng(1,:)=Qam_sym_ifft_new2(tgtRng(1,:)).*exp(1i*2*pi*doppler_e
ffect(1).*t);%*tgtPow(1);%%Incorporating Doppler effect
Qam_sym_ifft_new2(tgtRng(2,:)=Qam_sym_ifft_new2(tgtRng(2,:)).*exp(1i*2*pi*doppler_e
ffect(2).*t);%*tgtPow(2);%%Incorporating Doppler effect
Qam_sym_ifft_new2(tgtRng(3,:)=Qam_sym_ifft_new2(tgtRng(3,:)).*exp(1i*2*pi*doppler_e
ffect(3).*t);%*tgtPow(3);%%Incorporating Doppler effect
SignalFFT=abs(fft(Qam_sym_ifft_new2,pFFT,2)); %%% Zak transformation
temp3=[temp3 SignalFFT(tgtRng(1,:))];
% temp4=[temp4 SignalFFT(tgtRng(2,:))];
% temp5=[temp5 SignalFFT(tgtRng(3,:))];
Qam_sym_ifft_new3=cat(2,Qam_sym_ifft_new3, SignalFFT);
end

%%-----%%multiple target generation-end %%-----
Qam_sym_ifft_new4=reshape(temp3,pFFT,Nrf);
% Qam_sym_ifft_new6=reshape(temp4,pFFT,Nrf);
% Qam_sym_ifft_new7=reshape(temp5,pFFT,Nrf);
Qam_sym_ifft_new5=reshape(Qam_sym_ifft_new3,M,pFFT,Nrf);
figure,mesh((Qam_sym_ifft_new4));
title('Target detection after ZAK tranformation');
xlabel('Target AoA');
ylabel('Doppler Bin');
%figure,mesh(20*log10((Qam_sym_ifft_new5(:,5)))); %%% need Angle of Arrival

```

```
figure, mesh((Qam_sym_ifft_new5(:, :, 4))); %%% need Angle of Arrival  
ylim([1 512]);  
title('Target detection');  
xlabel('Doppler Bin');  
ylabel('Target Range in meters');
```